Supporting Information

Achieving efficient urea electrosynthesis through improving the coverage of crucial intermediate across broad nitrate concentrations

Yaodong Yu [a], Yuyao Sun [a], Jiani Han [a,b], Yujia Guan [a], Hongdong Li [a], Lei Wang [a] and Jianping Lai [a,*]

[a]Key Laboratory of Eco-chemical Engineering, Key Laboratory of Optic-electric Sensing and Analytical Chemistry of Life Science, Taishan Scholar Advantage and Characteristic Discipline Team of Eco Chemical Process and Technology, College of Chemistry and Molecular Engineering, Qingdao University of Science and Technology, Qingdao 266042, P. R. China

[b]Shandong Engineering Research Center for Marine Environment Corrosion and Safety Protection, College of Environment and Safety Engineering, Qingdao University of Science and Technology, Qingdao 266042, P. R. China

Experimental Section

Materials. Ruthenium acetylacetonate (97%, Macklin), Copper powder (Cu, 99.9%, Aladdin), Bismuth powder (Bi, 99.9%, Aladdin), Potassium nitrate (KNO_3, AR≥99.0%, Sinopharm), Potassium bicarbonate ($KHCO_3$, AR, 99.5%, Macklin), Carboxylated multi-walled carbon nanotubes (>95%, Aladdin). Iron chloride (99.9%, Aladdin), Diacetylmonoxime (>98%, Aladdin), Thiosemicarbazide (AR, 99%, Aladdin), Sodium hydroxide (NaOH, 97%, Aladdin), Salicylic acid (AR, 99.5%, Aladdin), Sodium citrate (98%, Aladdin), Sodium hypochlorite (NaClO, effective chlorine, >30%, Macklin), Sodium nitroferricyanide dihydrate (AR, 99.0%, Aladdin), p-dimethylaminobenzaldehyde (98%, Aladdin), 4-Aminobenzenesulfonamide (>98%, Sigma-Aldrich), N-(1-naphthyl) ethylenediamine dihydrochloride, (AR, 98%, Aladdin), Phosphoric acid (AR, >85%, Aladdin), H_2SO_4, HCl and C_2H_5OH were purchase from Sinopharm. Nafion solution (5%) was purchase from Sigma-Aldrich.

High pure CO_2 (99.999%) come from Qingdao Deyi Gas Company. The deionized water in the experiment is always ultrapure water (18.2 MΩ·cm).

Synthesis of Ru-Cu_9Bi/CNT. All catalysts were synthesized using a solvent-free microwave method. $Ru(acac)_2$ (5 mg), Cu powder (30 mg), Bi powder (15 mg) and carboxylated MWCNT (25 mg) were mixed in a mortar and ground evenly. Put the mixture into a 10 mL quartz vial. Then it was placed in a household microwave oven (Midea, PM2001) and reacted for 30 s with a power of 1 kW. The synthesis is initiated at room temperature and normal atmospheric pressure. The reaction mixture was then washed and centrifuged with ethanol. Finally, the product was dried overnight in a 60 ◦C oven to obtain a black powder. Ru-CuBi/CNT and Ru-Cu_3Bi/CNT were synthesised as described above. The difference is that the mass ratio of Cu to Bi was changed to 1:1 and 3:1.

Synthesis of Cu_9Bi/CNT. The synthesis method is similar to that of Ru-Cu_9Bi/CNT, with the difference that $Ru(acac)_2$ is not added.

Synthesis of Ru-Cu_{19}/CNT. The synthesis method is similar to that of Ru-Cu_9Bi/CNT. The difference is that the mass of Cu powder was changed to 45 mg and Bi powder was not added.

Synthesis of Ru-Bi_{19}/CNT. The synthesis method is similar to that of Ru-Cu_9Bi/CNT. The difference is that the mass of Bi powder was changed to 45 mg and Cu powder was not added.

Characterization. Scanning electron microscopy (SEM) images were obtained by Hitachi, S-8200. The transmission electron microscope (TEM) and high-resolution TEM (HRTEM) of the catalyst were tested using FEI Tecnai-G2 F30 at an accelerating voltage of 80 KV. Powder X-ray diffraction (XRD) spectra were recorded on an X'Pert-Pro MPD diffractometer with Cu Kα radiation at 40 KV and 40 mA. X-ray photoelectron spectroscopy (XPS) analysis was performed with an Axis Supra spectrometer using a monochromatic Al Kα source at 15 mA and 14 kV. All the electrochemical performances of the as-synthesized samples were carried out on an electrochemical station (CHI 760E). The ^{1}H NMR spectrum was recorded on a Bruker 500 with Probe TXI at the temperature of 25 ℃ using a 3 mm tube. The electrolyte after electrolysis was collected, lyophilized, and further dissolved in 1 M HCl

solution (D_2O/H_2O mixed solution). In-situ fourier transform infrared (FTIR) spectra of the materials were recorded by Nicolet iS50 FTIR spectrometer (Thermo Fisher Scientific, USA).

Electrochemical measurements. All electrochemical characterizations were performed using a CHI 760E workstation coupled with a three-electrode system in a two-compartment cell separated by Nafion 117 membrane. And the Nafion membrane was heated at 80 ℃ in (5 wt%) H_2O_2 aqueous solution for 1 h to remove the organic impurities in the membrane. Secondly, wash the membrane repeatedly with deionized water, soak it in deionized water at 80 ℃ and boil it for 1 h to completely remove the residual H_2O_2. Immerse the membrane in 1.0 mol L^{-1} H_2SO_4 solution at 80 ℃ for 1 h, and convert the membrane into H^+type through ion exchange. Finally, it is rinsed repeatedly with deionized water and soaked in deionized water at 80 ℃ for heat treatment for 1 h to completely remove the residual H_2SO_4 in the membrane. To avoid contamination with nitrogen-containing species in the air, electrodes were used either immediately after preparation or kept in vacuum before being used in electrochemical experiments. The prepared catalyst was used as the working electrode, a graphite rod, and the saturated calomel electrode (SCE) with a saturated KCl electrolyte as the counter electrode and reference electrode, respectively. Potential without iR-compensated were converted to RHE scale via the following equation: E (vs. RHE) = E (vs. SCE) + 0.0591×pH + 0.241 (pH = 6.8 in CO_2-saturated electrolyte in 0.1 M $KHCO_3$ + 0.1 M KNO_3). The catalyst ink for working electrode was prepared by dispersing 1 mg of catalyst in a mixed solution of 30 μL Nafion (0.5 wt%), 500 μL ethanol and 470 μL water followed by sonication for 30 minutes. Mass loading of 0.1 mg cm^{-2} was used for electrochemical study. All experiments were carried out at room temperature (25℃). To remove the impurities in the inlet gas, such as NO_x, the pre-purification of high-purity CO_2 (purity 99.99%) by passing through a saturator filled with 0.05 M NaOH and a saturator filled with 0.05 M H_2SO_4 solution to remove any possible contaminants. Before carrying out all the electrochemical characterizations, the 0.1 M $KHCO_3$ + 0.1 M KNO_3 electrolyte solution was purged with CO_2 for 30 min. Cyclic voltammetry (CV) test was carried out at a scan rate of 50 mV s^{-1} ranging from 0-0.2 V (vs. RHE).

Linear sweep voltammetry (LSV) was also conducted at a scan rate of 5 mV s^{-1}. Chronoamperometric tests were then conducted at different potentials and CO_2 was continuously fed into the cathodic cell during the experiments. The recycle test was to perform ten consecutive cycles of chronoamperometric runs without changing the catalysts at -0.4 V vs. RHE. Electrochemical impedance spectroscopy (EIS) was conducted at a frequency range from 100 kHz to 1 Hz with a 10 mV AC signal amplitude at -0.4 V vs. RHE on a PAR-STAT 2273 test system.

Product quantification. Gas products were analyzed using gas chromatography (GC 7900) equipped with a thermal conductivity detector (TCD) and flame ionization detector (FID). Argon (99.999%) was used as a carrier gas. H_2 is detected by a TCD, and CO is detected by an FID equipped with a mechanized.

Calculation of turnover frequency (TOF). Owing to the bulk nature of the catalysts, we selected an electrochemical method to obtain the TOF values of each sample. Nearly all the surface-active sites were assumed to be accessible by the electrolyte, and then the TOF values could be calculated by the following equation:

$$TOF = \frac{I}{16 \times F \times n}$$

where I, n, and F are current during linear sweep measurement, the number of active site numbers, and the Faraday constant, respectively. The factor of 1/16 is because NO_3^- reduction requires sixteen electrons to produce a urea molecule from two nitrate radicals. The values (n) were calculated from the CV data in the potential range from -0.2 V to +0.6 V (vs. RHE) in 1 M phosphate buffer (pH = 7.4) at a scan rate of 50 mV/s. Since it is very difficult to assign the observed peaks to a given redox couple, the surface-active sites are nearly in a linear relationship with the integrated voltametric charges (cathodic and anodic) over the CV curves. Assuming a one-electron process for both reduction and oxidation, we can evaluate the upper limit of the active site number according to the following formula:

$$n = \frac{Q_{CV}}{2 \times F}$$

where the Q represents the whole charge of the CV curve.

ECSA measurements. To estimate the ECSA values of the materials, double-layered capacitance (C_{dl}) was measured using a simple cyclic voltammetry method. Here, the potential window has been chosen to be outside the material's possible faradic region (0.52~0.62 V vs RHE) and CV was recorded at various scan rates ranging from 20-100 mV s^{-1}. The capacitive current density, ΔJ/2, was linearly related to the scan rate and the double layer capacitance (Cdl) was calculated from the slopes of these straight lines. C_{dl} was further converted into ECSA using the specific capacitance value (~0.04 mF) of a standard 1.0 cm^{-2} surface.

$$\text{ECSA} = \frac{C_{dl}}{C_s}$$

$$\text{Cs} = 0.04 \text{ mF cm}^{-2}$$

Determination of urea concentration by diacetyl monoxime method. The urea concentration was determined by the diacetyl monoxime method [Clin Chim Acta., 1980, 107, 3-9]. 10 mL concentrated phosphoric acid was mixed with 30 mL of concentrated sulfuric acid and 60 mL distilled water, then 10 mg $FeCl_3$ was dissolved in the above solution, denoted as the acid-ferric solution. Then, 0.5 g of diacetyl monoxime (DAMO) and 10 mg of thiosemicarbazone (TSC) were dissolved in distilled water and diluted to 100 mL, denoted as DAMO-TSC solution. Typically, 1 mL of the sample solution was removed from the cathodic chamber. Afterward, 1 mL of DAMO-TSC solution and 2 mL of acid-ferric solution was added into 1 mL of sample solution. Next, the mixed solution was heated to 100 ℃ and maintained at this temperature for 15 min. When the solution cooled to 25 ℃, the UV-Vis absorption spectrum was collected at a wavelength of 525 nm. The concentration-absorbance curve was calibrated using standard urea solution for a series of concentrations. The fitting curve shows good linear relation of absorbance value with urea concentration by three times independent calibration tests.

Calculation of Faradaic efficiency (FE) and urea formation rate. The FE for urea electrosynthesis was defined as the amount of electric charge used for producing urea divided by the total charge passed

through the electrodes during the electrolysis. Assuming 16 electrons were needed to produce one urea molecule, the FE was calculated according to the following equation:

$$FE = 16 * F * C_{urea} * V/(60.06 * Q)$$

The rate of formation of urea was calculated using the following equation:

$$Urea\ yield\ rate = C_{urea} * V/(60.06 * t * m_{cat})$$

Where F is Faraday constant (96485 C mol^{-1}), C_{urea} is the measured mass concentration of urea; V is the volume of the cathodic reaction electrolyte; Q is the electric quantity of charge passing through; t is the time for which the potential was applied; S is the electrode area entering the electrolyte.

Determination of NH_3 concentration by indophenol blue method. The produced NH_3 was spectrophotometrically determined by the indophenol blue method [Nat Mater. 2013, 12, 836-841]. 1.0 M NaOH solution of 5 wt% salicylic acid and 5 wt% sodium citrates, recorded as acid-base Typically, 1 mL of the sample solution was removed from the cathodic chamber. Afterward, 1 mL of acid-base, followed by 0.5 mL NaClO solution (0.05 M) and 100 μL of an aqueous solution of sodium nitroferricyanide (1 wt%) were added. After standing at room temperature for 2 h, the UV-Vis absorption spectrum was collected at a wavelength of 655 nm. The concentration-absorbance curve was calibrated using a standard NH_4Cl solution for a series of concentrations. The fitting curve shows good linear relation of absorbance value with NH_4Cl concentration by three times independent calibration tests.

Calculation of Faradaic efficiency (FE) of NH_3. The FE for NRR was defined as the amount of electric charge used for producing NH_3 divided by the total charge passed through the electrodes during the electrolysis. Assuming 8 electrons were needed to produce one NH_3 molecule, the FE was calculated according to the following equation:

$$FE = 8 * F * C_{NH3} * V/(17 * Q)$$

Where F is Faraday constant (96485 C mol^{-1}), C_{NH3} is the measured mass concentration of NH_3; V is

the volume of the cathodic reaction electrolyte; Q is the electric quantity of charge passing through.

Determination of NO_2^- concentration by indophenol blue method. 20 g p-aminobenzenesulfonamide was dissolved into a mixed solution of 250 mL water and 50 mL of phosphoric acid, and 1 g of N-(1-naphthyl)-ethylenediamine dihydrochloride was then added. For the detection, 0.1 mL of NO_2^- of color reagent was added into 5 mL of electrolyte solution and stood for 20 min. It was then characterized by UV-vis spectrophotometer. The absorbance at 540 nm is assigned to NO_2^-. The calibration curve of standard NO_2^- was also plotted to determine the NO_2^- concentration.

Calculation of Faradaic efficiency (FE) of NO_2^-. The FE for NRR was defined as the amount of electric charge used for producing NO_2^- divided by the total charge passed through the electrodes during the electrolysis. Assuming 2 electrons were needed to produce one NO_2^- molecule, the FE was calculated according to the following equation:

$$FE = 2 * F * C_{NO2\_} * V/(47 * Q)$$

Where F is Faraday constant (96485 C mol-1), C_{NO2-} is the measured mass concentration of NO_2^-; V is the volume of the cathodic reaction electrolyte; Q is the electric quantity of charge passing through.

Determination of N_2H_4 concentration by Watt and Chrisp method. The produced N_2H_4 was spectrophotometrically determined by the Watt and Chrisp. 2 mL solution that removed from the electrocatalysis cell was added 2 mL color reagent. The color reagent contains 5.99 g p-$C_9H_{11}NO$, 30 mL HCl and 300 mL C_2H_5OH. After standing at room temperature for 15 min, UV-Vis absorption spectra were measured using an UV-Vis spectrophotometer at 455 nm. The standard curve was calibrated using standard N_2H_4 solutions with series of concentrations.

Urease decomposition method: Add 0.2 mL of 5 mg mL^{-1} urease solution to 1.8 mL of urea electrolyte and react at 45℃ for 40 min. One urea molecule is broken down by urease into CO_2 and two NH_3 molecules. After decomposition, the concentration of NH_3 in the original urine electrolyte was measured using the indophenol blue method, while the concentration of NH_3 in the electrolyte

after enzymatic decomposition was also measured.

Calculation Setup: We carried out all the DFT calculations in the Vienna *ab initio* simulation (VASP5.4.4) code. The exchange-correlation is simulated with PBE functional and the ion-electron interactions were described by the PAW method. The vdWs interaction was included by using empirical DFT-D3 method. Cu (001), Mo (001), and the Cu and Mo doped four layers of Ga (021) surface were employed to simulate the the reaction of CO and N_2 to form $CO(NH_2)_2$. Atoms in the upper two layers of the surface are allowed to move freely while the bottom two layers of surface are fixed to simulate the surface of structure. The lattice parameter is a=10.71 Å, b=1.60 Å while the α=β=90°，γ=74.29°. Along the z direction, a 25 Å vacuum layer is added to the surface to adsorb the reactant and to avoid the interactions between periodic structures. The Monkhorst-Pack-grid-mesh-based Brillouin zone k-points are set as 2×2×1 for all periodic structure with the cutoff energy of 400 eV. The convergence criteria are set as 0.02 eV A^{-1} and 10^{-5} eV in force and energy, respectively.

The free energy calculation of species adsorption (ΔG) is based on following model.

$$\Delta G = \Delta E + \Delta E_{ZPE} + \Delta H_{0\to T} - T\Delta S \quad (1)$$

Herein ΔE, ΔE_{ZPE}, and ΔS respectively represent the changes of electronic energy, zero-point energy, and entropy that caused by adsorption of intermediate. The $\Delta H_{0\to T}$ refers to the change in enthalpy when heating from 0K to T K.

Figures

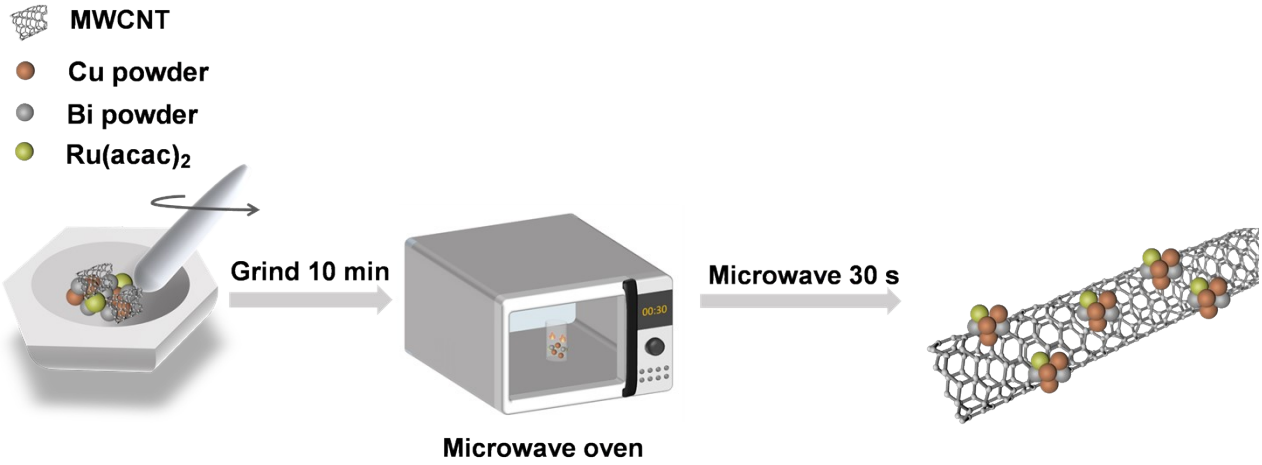

Figure S1. Schematic diagram illustrating the synthetic procedure of Ru-Cu_xBi_y/CNT.

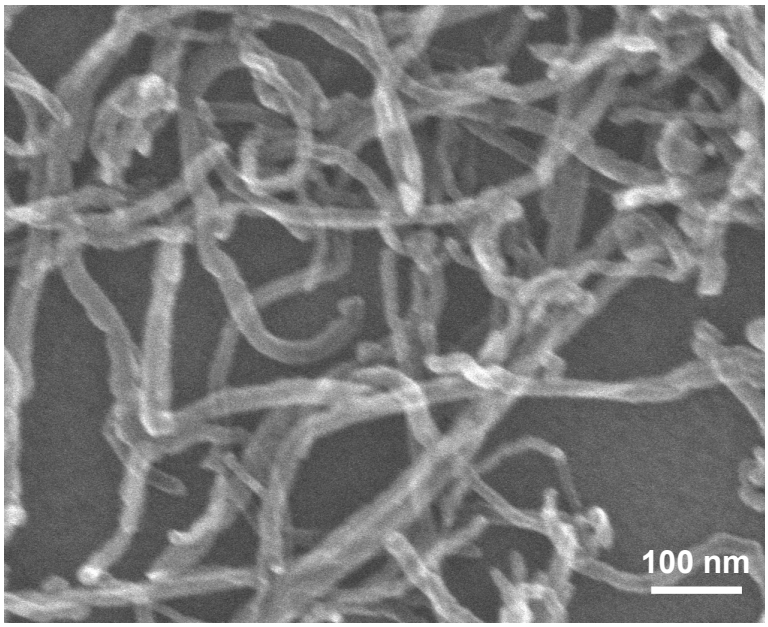

Figure S2. The SEM image of carboxylated MWCNT.

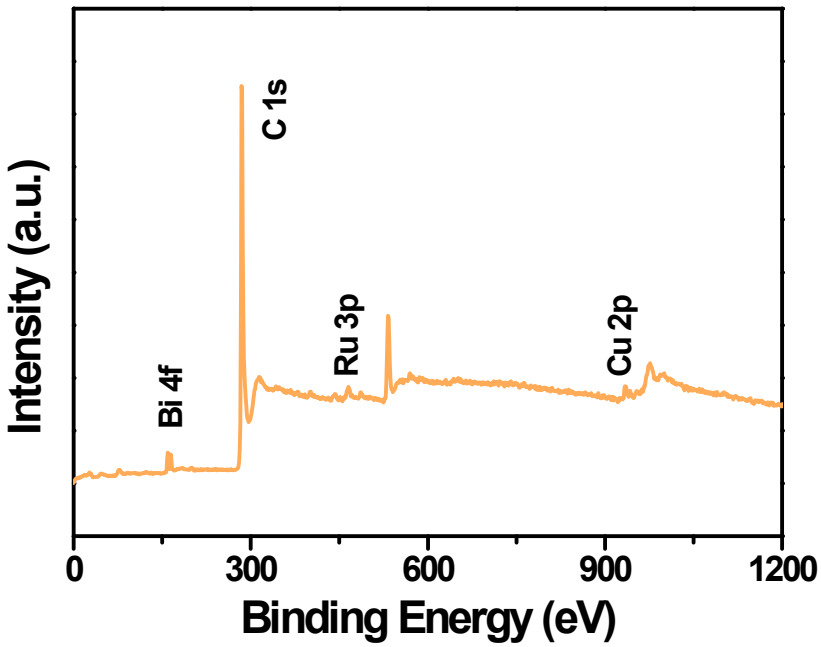

Figure S3. XPS spectra of Ru-Cu_9Bi/CNT.

Figure S4. The optical photograph of the H-cell system for urea electrosynthesis testing.

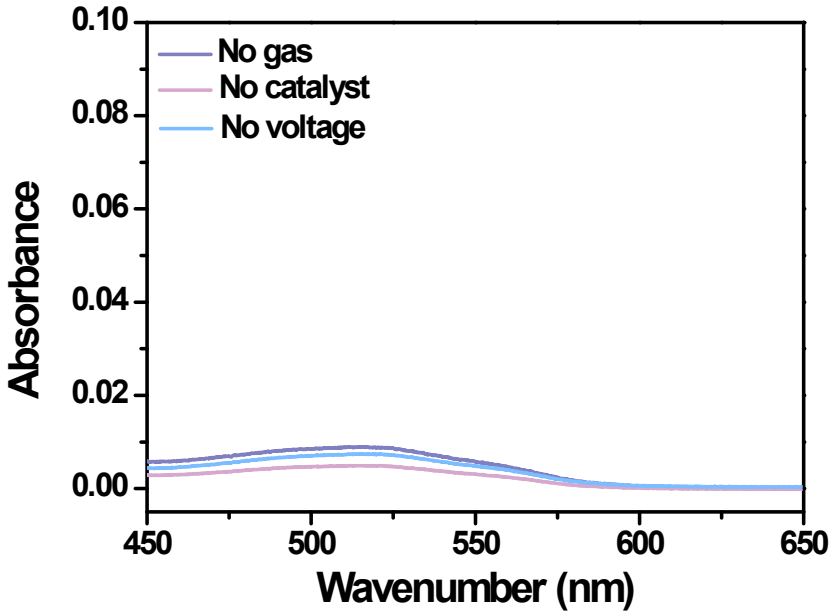

Figure S5. UV-vis absorption spectra tested in 0.1 M $KHCO_3$ + 0.1 M KNO_3.

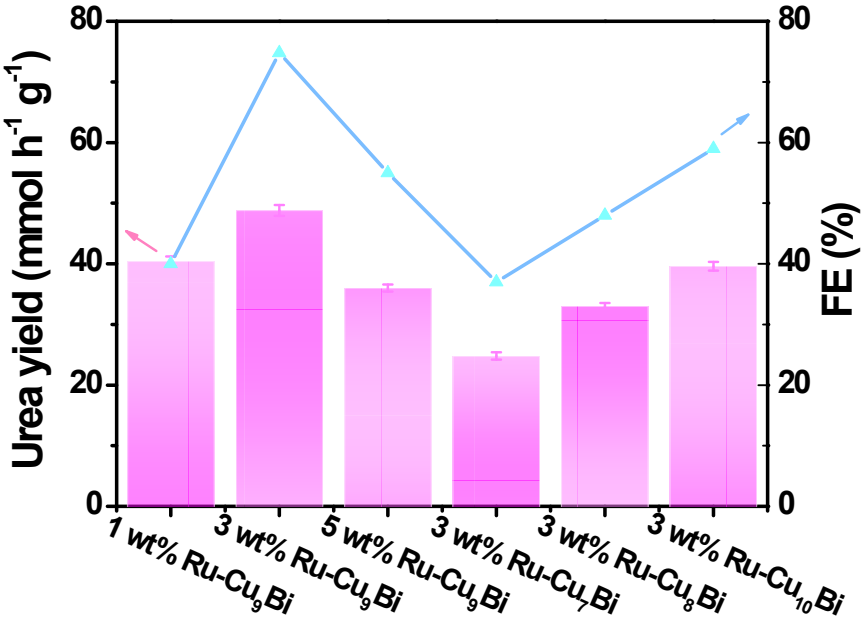

Figure S6. Comparison of urea yield of Ru-Cu_xBi_y/CNT catalyst with different amount of Ru-doping and mass ratio of Cu to Bi.

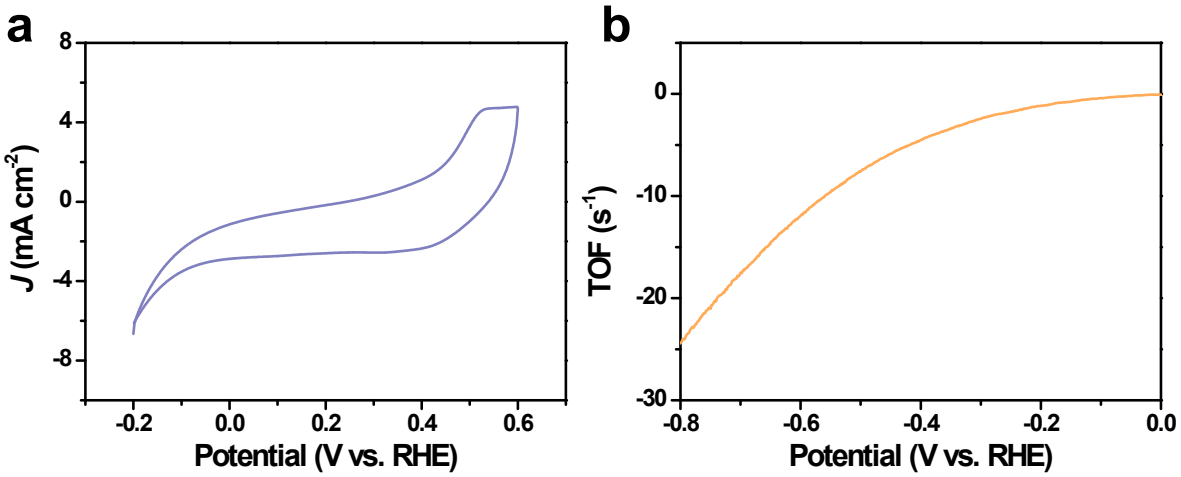

Figure S7. (a) The CV and (b) TOF at -0.4 V vs. RHE of Ru-Cu_9Bi/CNT.

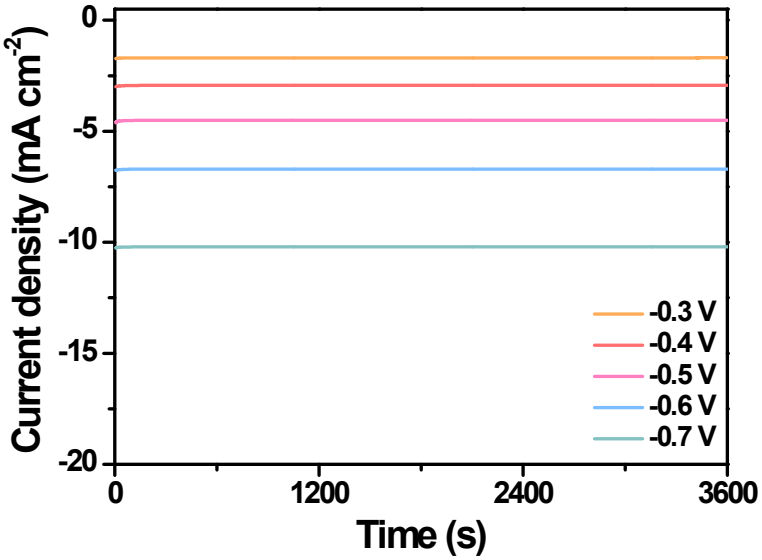

Figure S8. Dependence of current density on time for Ru-Cu_9Bi/CNT in CO_2-saturated 0.1 M $KHCO_3$ + 0.1 M KNO_3 solution.

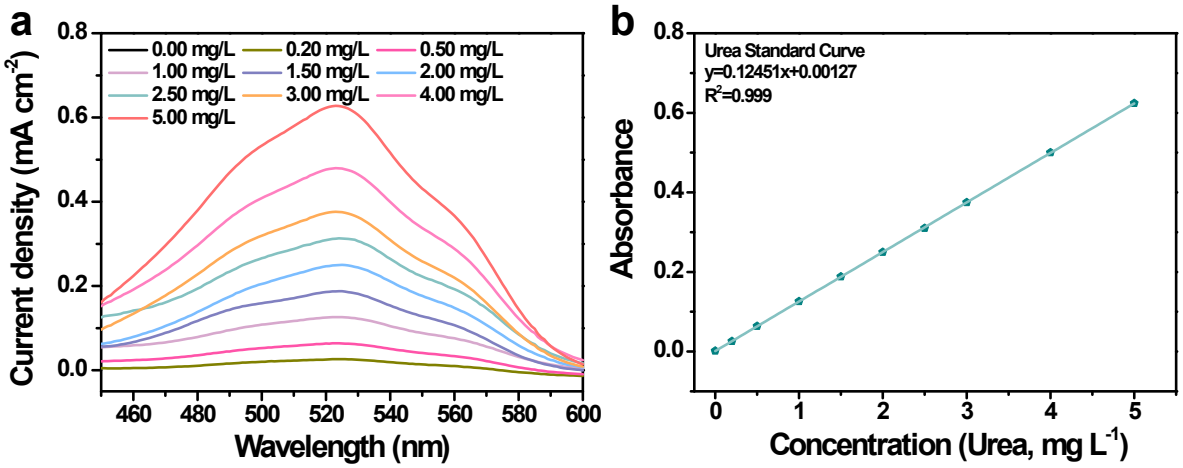

Figure S9. (a) UV-vis curves and (b) concentration-absorbance of urea solution with a series of standard concentration (0-5.0 μg mL^{-1}). The absorbance at 525 nm was measured by UV-vis spectrophotometer. The standard curve shows good linear relation of absorbance with urea concentration (R^2=0.999).

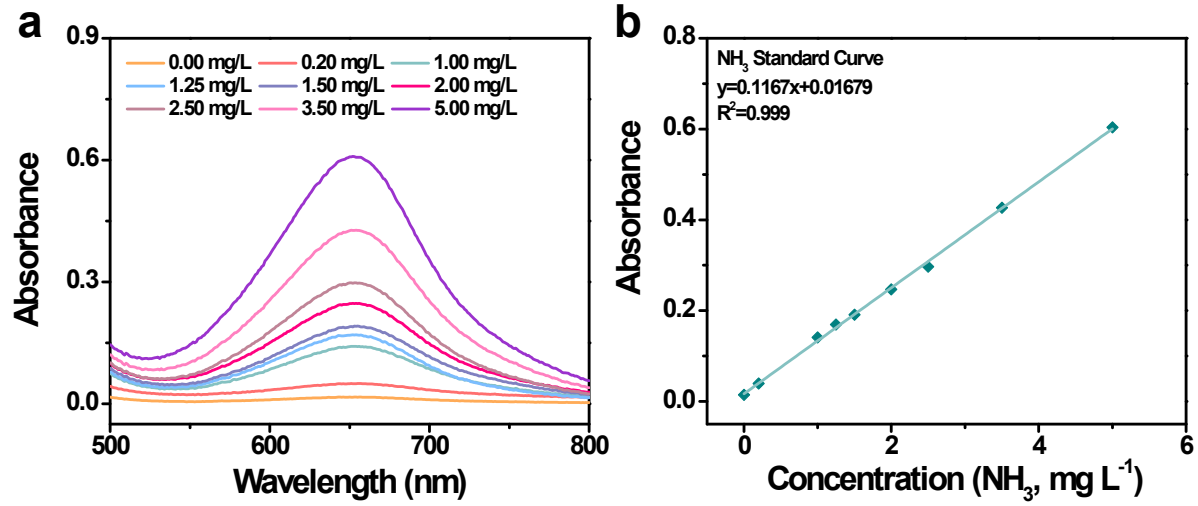

Figure S10. (a) UV-vis curves and (b) concentration-absorbance of NH_3 solution with a series of standard concentrations (0-5.0 μg mL^{-1}). The absorbance at 655 nm was measured by UV-vis spectrophotometer. The standard curve shows good linear relation of absorbance with NH_3 concentration (R^2=0.999).

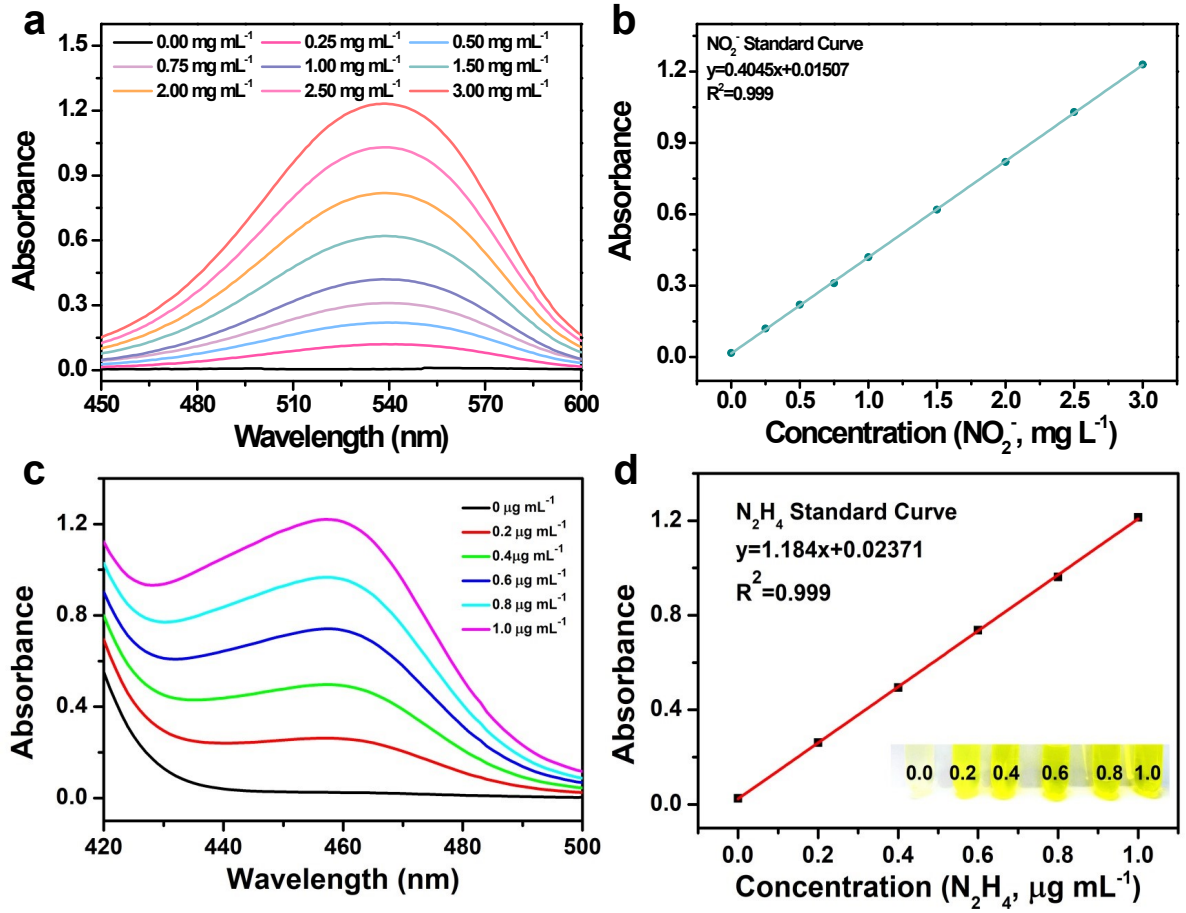

Figure S11. (a) UV-vis curves and (b) concentration-absorbance of NO_2^- solution with a series of standard concentrations (0-3.0 μg mL^{-1}). The absorbance at 540 nm was measured by UV-vis spectrophotometer. The standard curve shows good linear relation of absorbance with NO_2^- concentration (R^2=0.999). (c) UV-vis curves and (d) concentration-absorbance of N_2H_4 solution with a series of standard concentrations (0-1.0 μg mL^{-1}). The absorbance at 455 nm was measured by UV-vis spectrophotometer. The standard curve shows good linear relation of absorbance with N_2H_4 concentration (R^2=0.999).

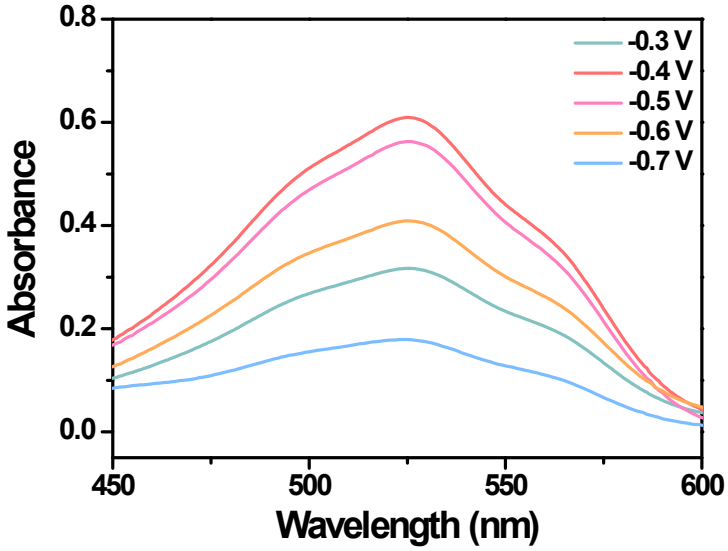

Figure S12. The UV test spectrum of urea of Ru-Cu_9Bi/CNT catalyst in 0.1 M $KHCO_3$ + 0.1 M KNO_3 solution.

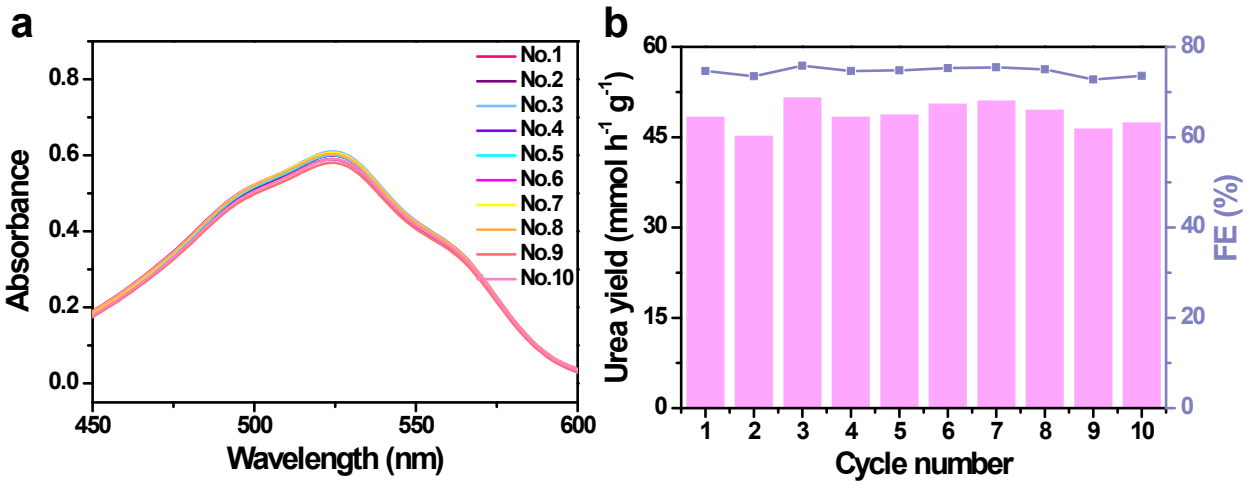

Figure S13. (a) The UV test spectrum of urea and (b) the Faradaic efficiency and urea yield of Ru-Cu_9Bi/CNT catalyst at -0.4 V vs. RHE during ten times recycling tests.

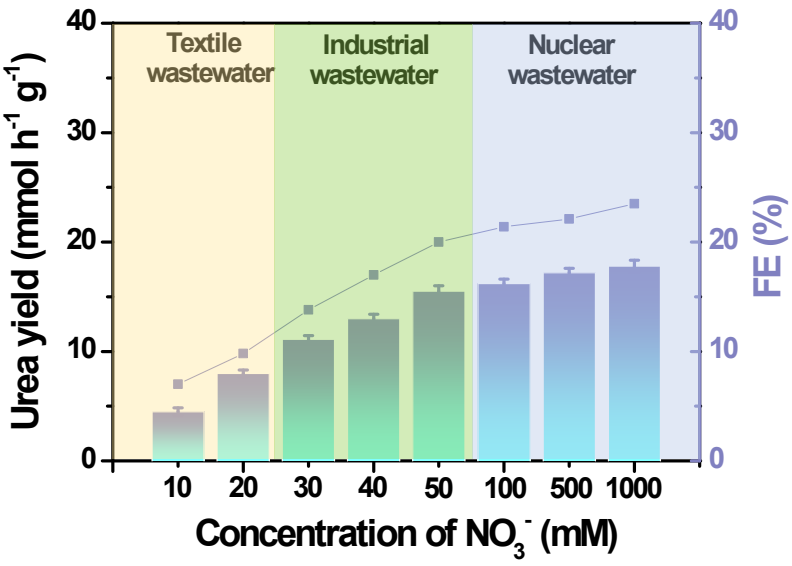

Figure S14. Urea yield and FE of Cu_9Bi/CNT in different concentration nitrate sources (contaminated textile wastewater, industrial wastewater, liquid nuclear wastes).

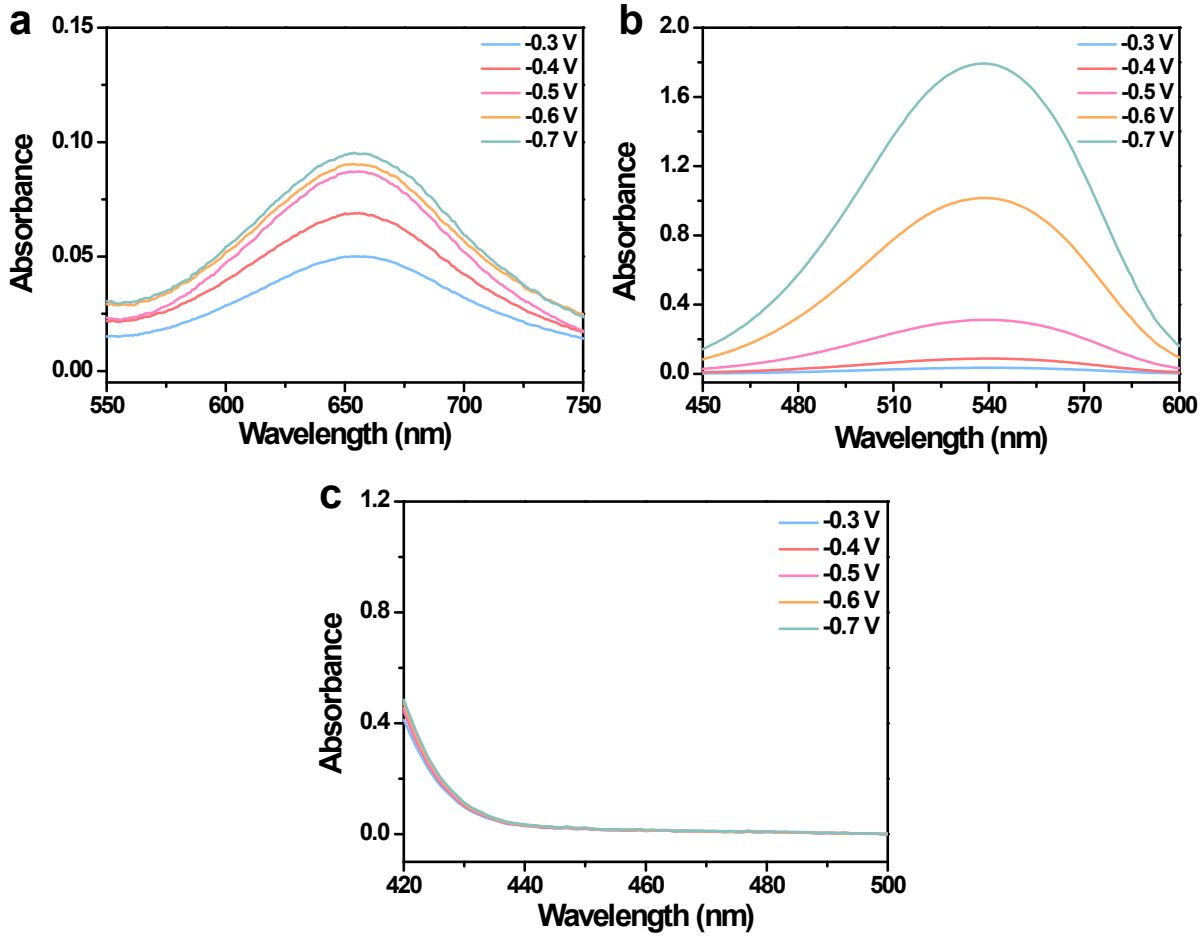

Figure S15. The UV test spectrum of (a) NH_3, (b) NO_2^- and (c) N_2H_4 of Ru-Cu_9Bi/CNT catalyst in 0.1 M $KHCO_3$ + 0.1 M KNO_3 solution.

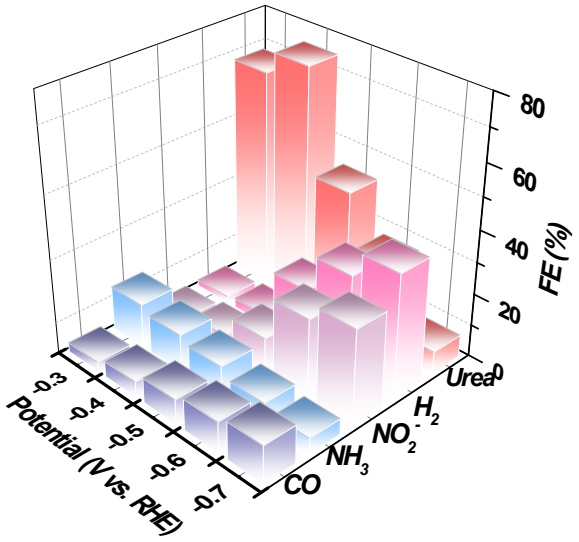

Figure S16. Product Faraday efficiency distribution of Ru-Cu_9Bi/CNT at different potentials.

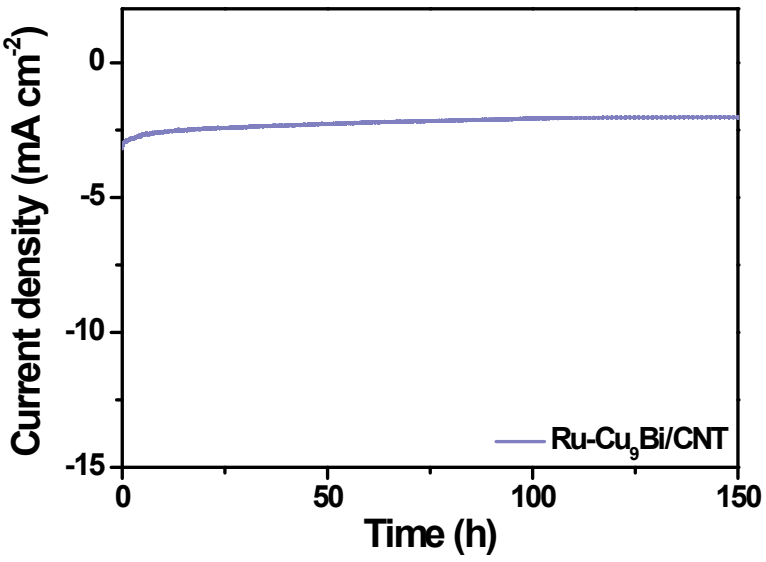

Figure S17. The chronoamperometric curves of Ru-Cu_9Bi/CNT at -0.4 V vs. RHE for 150 h in CO_2 saturated 0.1 M $KHCO_3$ + 0.1 M KNO_3 solution.

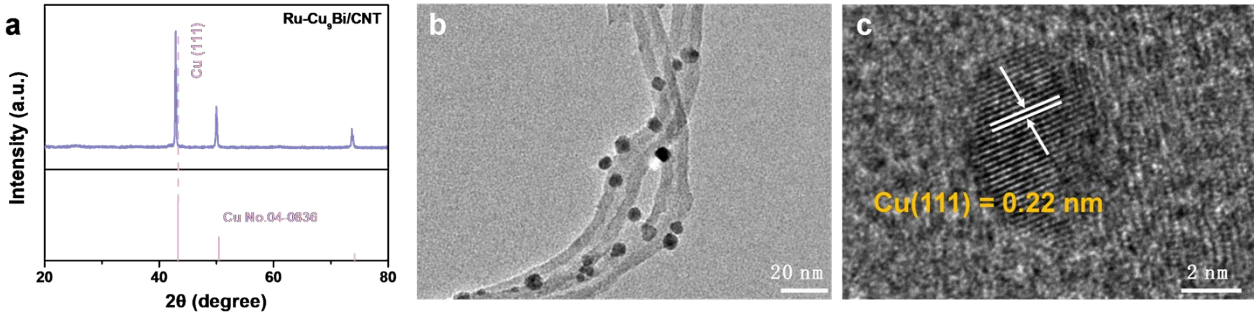

Figure S18. (a) XRD, (b) TEM and (c) HRTEM image of Ru-Cu_9Bi/CNT catalyst at -0.4 V vs. RHE after the reaction.

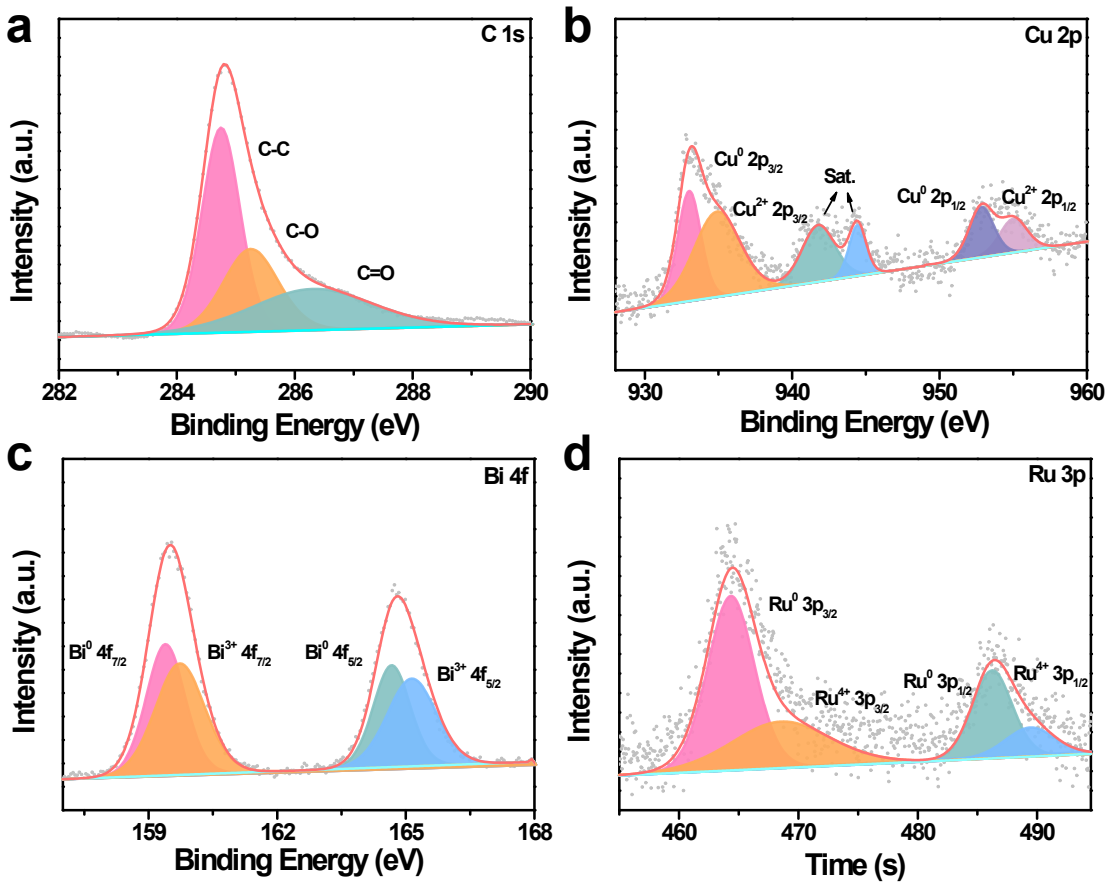

Figure S19. XPS spectra of Ru-Cu_9Bi/CNT. (a) C 1s, (b) Cu 2p, (c) Bi 4f, (d) Ru 3p.

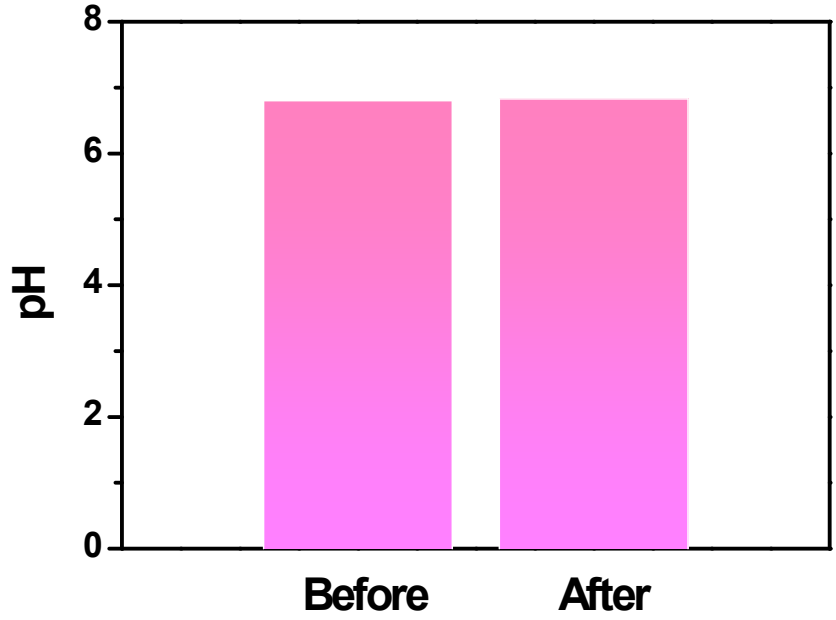

Figure S20. Comparison of pH before and after the reaction.

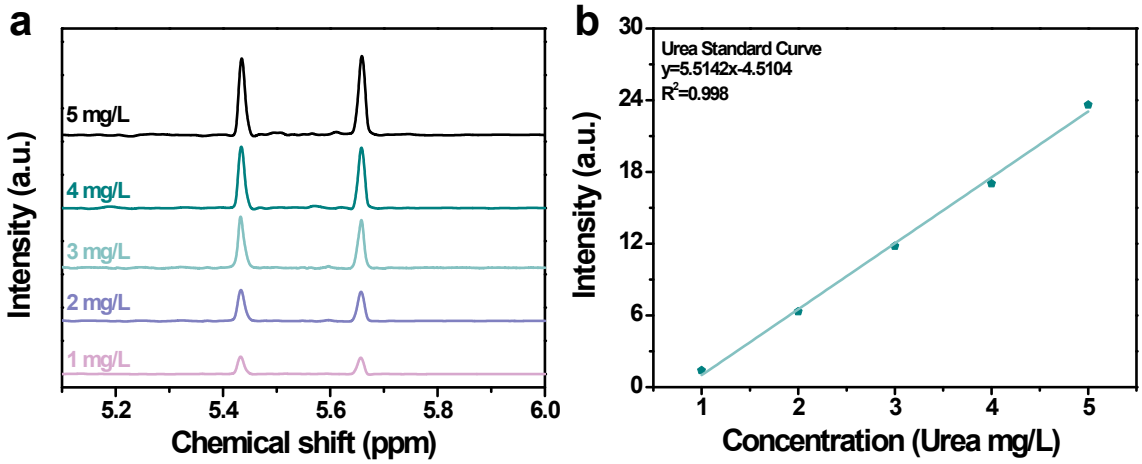

Figure S21. (a) ^{1}H NMR spectra of standard $^{15}NH_2CO^{15}NH_2$ solution with various concentrations of 0-5.0 μg mL^{-1}. (b) Integral area concentration linear relation calibrated using standard $^{15}NH_2CO^{15}NH_2$ solution.

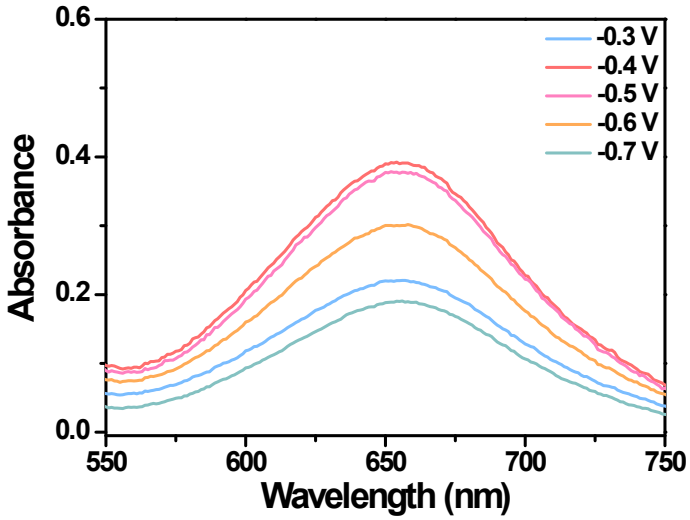

Figure S22. UV-vis absorption spectra of NH_3 after urease decomposition.

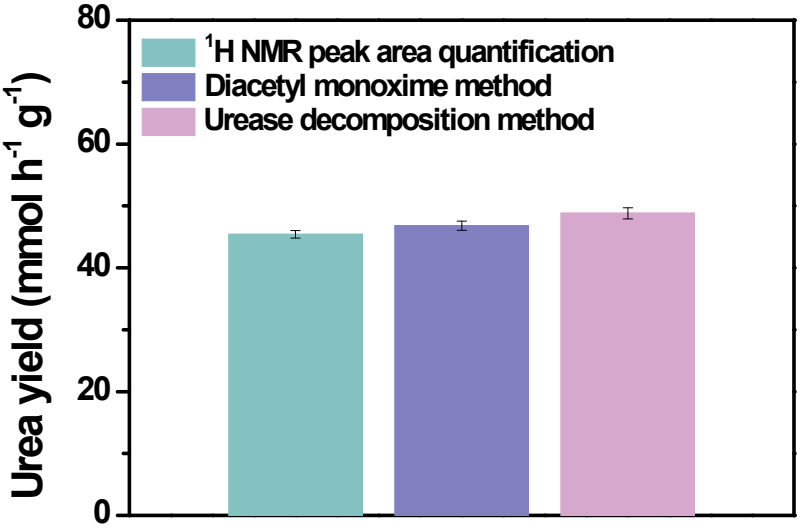

Figure S23. The urea yield rate of Ru-Cu_9Bi/CNT at -0.4 V vs. RHE detected by urease dissociation method, ^1H NMR peak area quantification and diacetyl monoxime method.

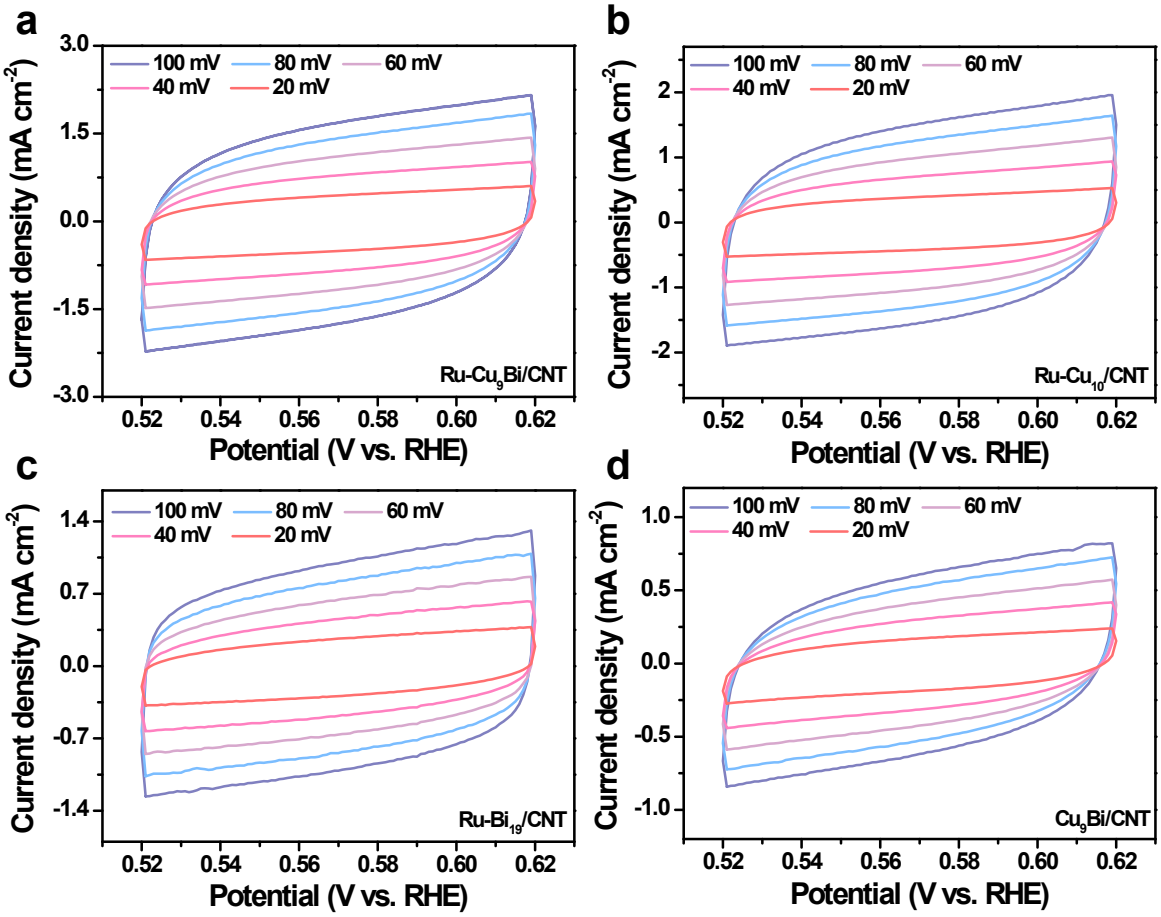

Figure S24. CV curves of (a) Ru-Cu_9Bi/CNT, (b) Ru-Cu_{10}/CNT, (c) Ru-Bi_{10}/CNT and (d) Cu_9Bi/CNT with different scan rates from 20 to 100 mV/s.

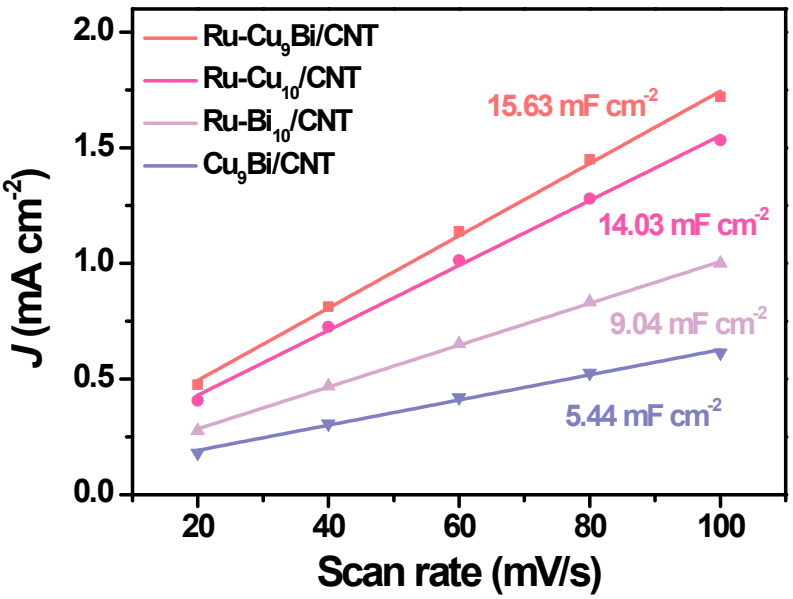

Figure S25. Capacitive current at middle potential of CV curves as function of scan rates for Ru-Cu_9Bi/CNT, Ru-Cu_{10}/CNT, Ru-Bi_{10}/CNT and Cu_9Bi/CNT catalysts.

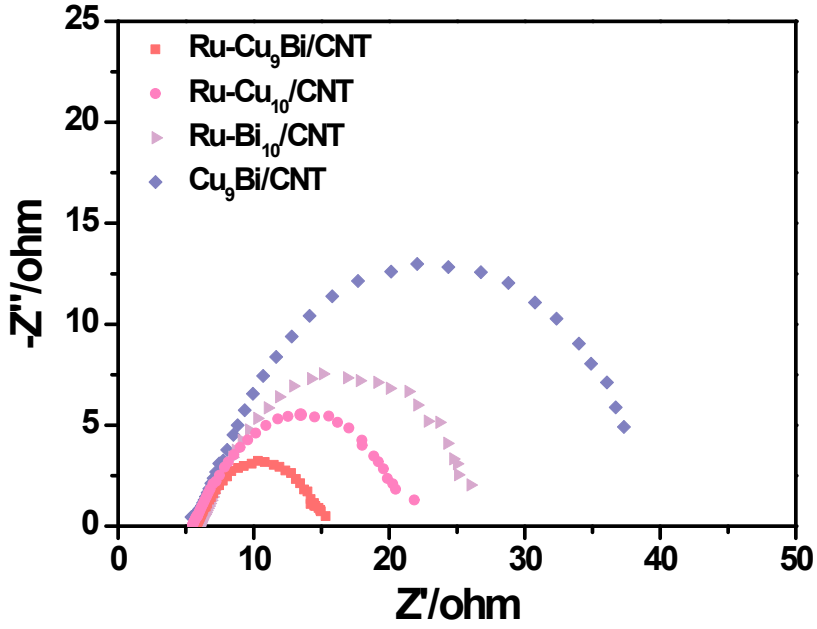

Figure S26. EIS Nyquist plots of Ru-Cu_9Bi/CNT, Ru-Cu_{10}/CNT, Ru-Bi_{10}/CNT and Cu_9Bi/CNT catalysts.

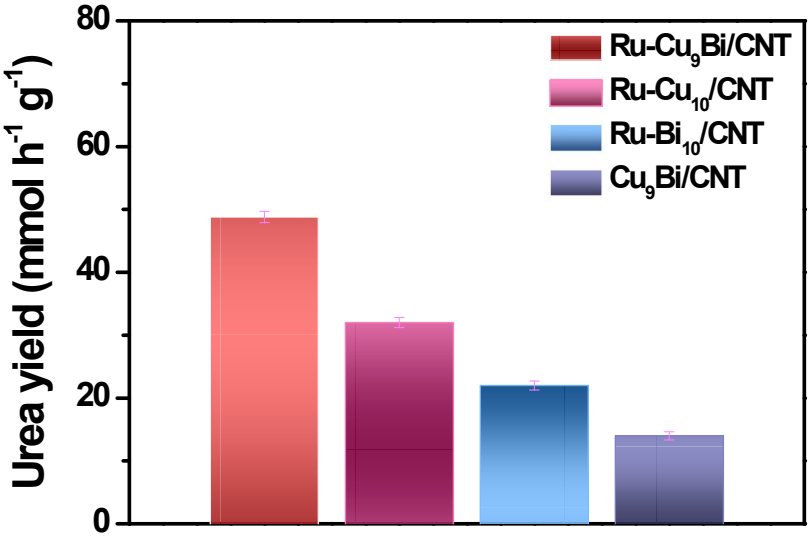

Figure S27. Urea yield of Ru-Cu_9Bi/CNT, Ru-Cu_{10}/CNT, Ru-Bi_{10}/CNT and Cu_9Bi/CNT in 0.1 M $KHCO_3$ + 0.1 M KNO_3 with CO_2 electrolyte at -0.4 V vs. RHE.

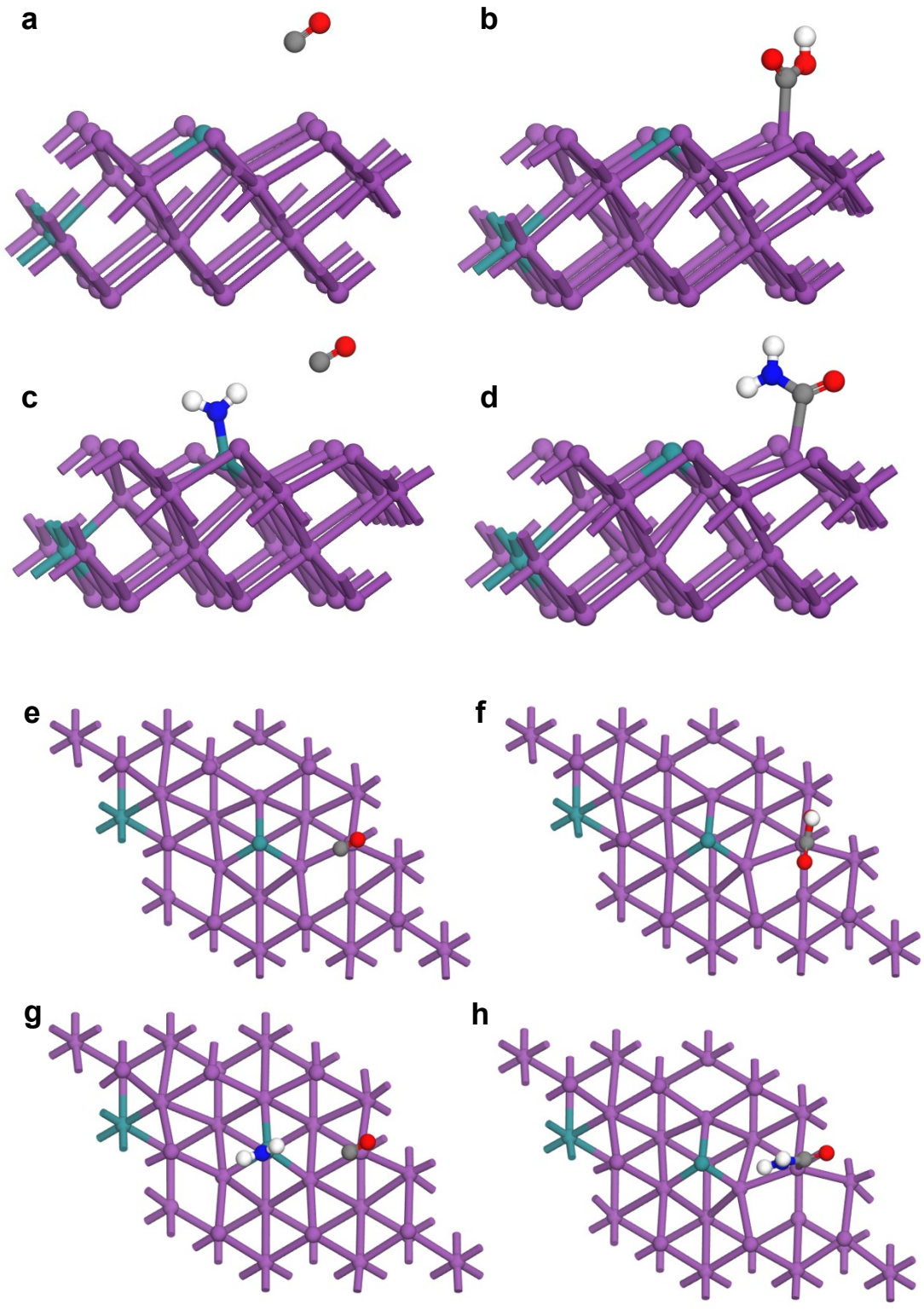

Figure S28. Ru-Bi_{10}/CNT (111) adsorption of (a, e) *CO, (b, f) *COOH, (c, g) *CO+*NH_2 and (d, h) *$CONH_2$. Side view (top) and top view (bottom). (Green: Ru, orange: Cu, purple: Bi, blue: N, red: O, white: H and gray: C, same as below.)

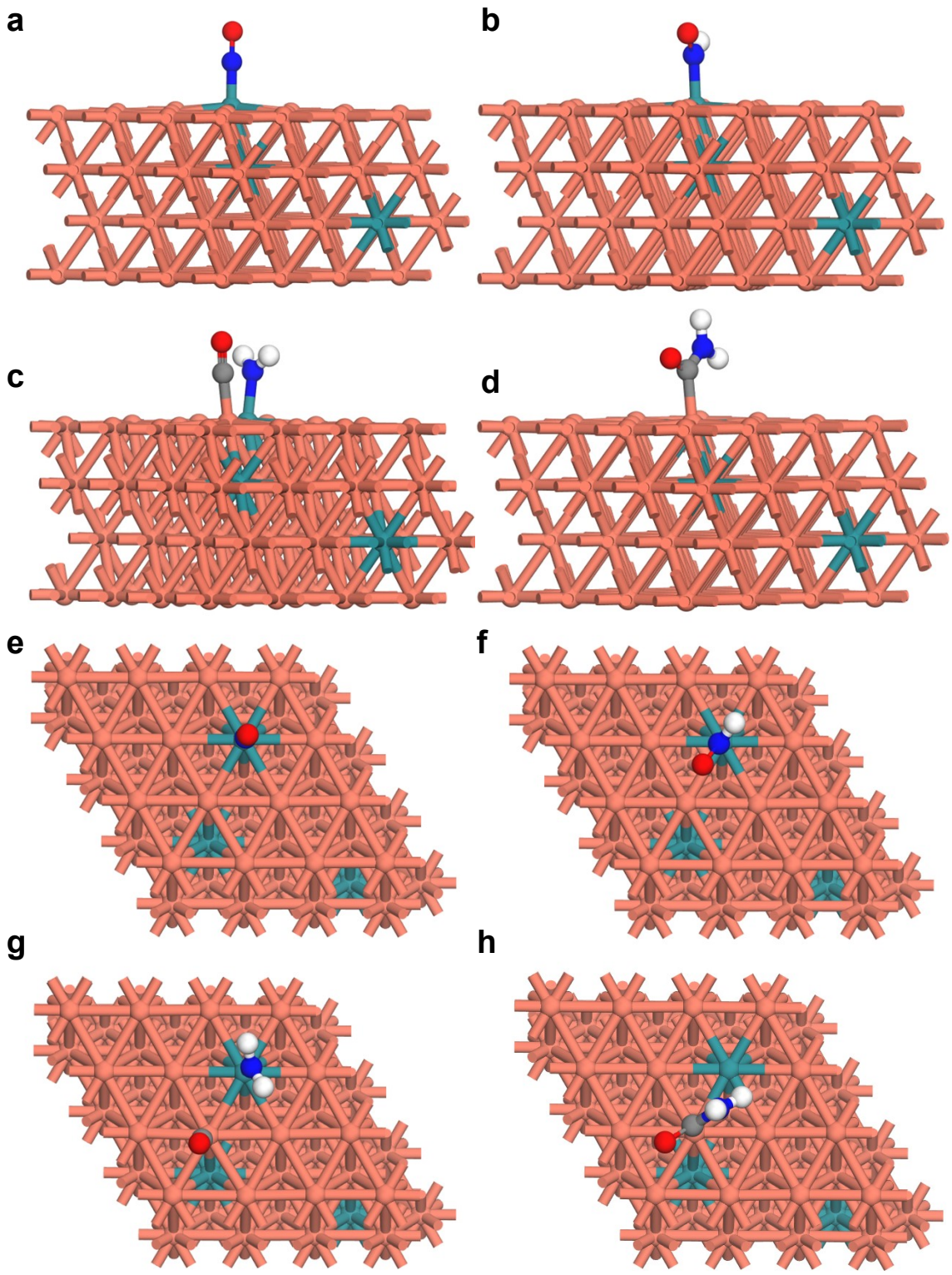

Figure S29. Ru-Cu_{10}/CNT (111) adsorption of (a, e) *NO, (b, f) *CHO, (c, g) *CO+*NH_2 and (d, h) *$CONH_2$. Side view (top) and top view (bottom).

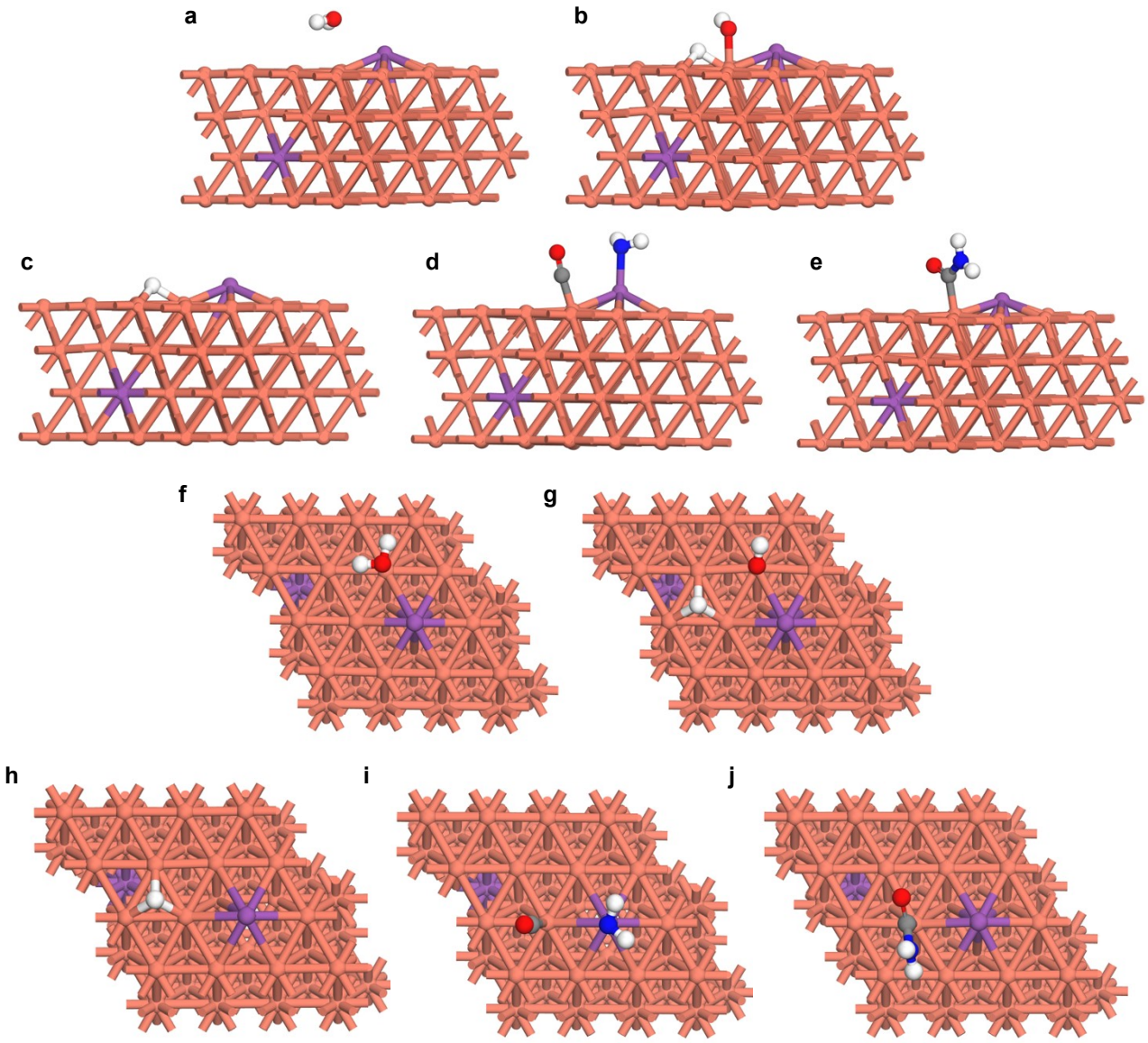

Figure S30. Cu_9Bi/CNT (111) adsorption of (a, f) *H_2O, (b, g) *H+*OH, (c, h) *H, (d, i) *CO+NH_2 and (e, j) *$CONH_2$. Side view (top) and top view (bottom).

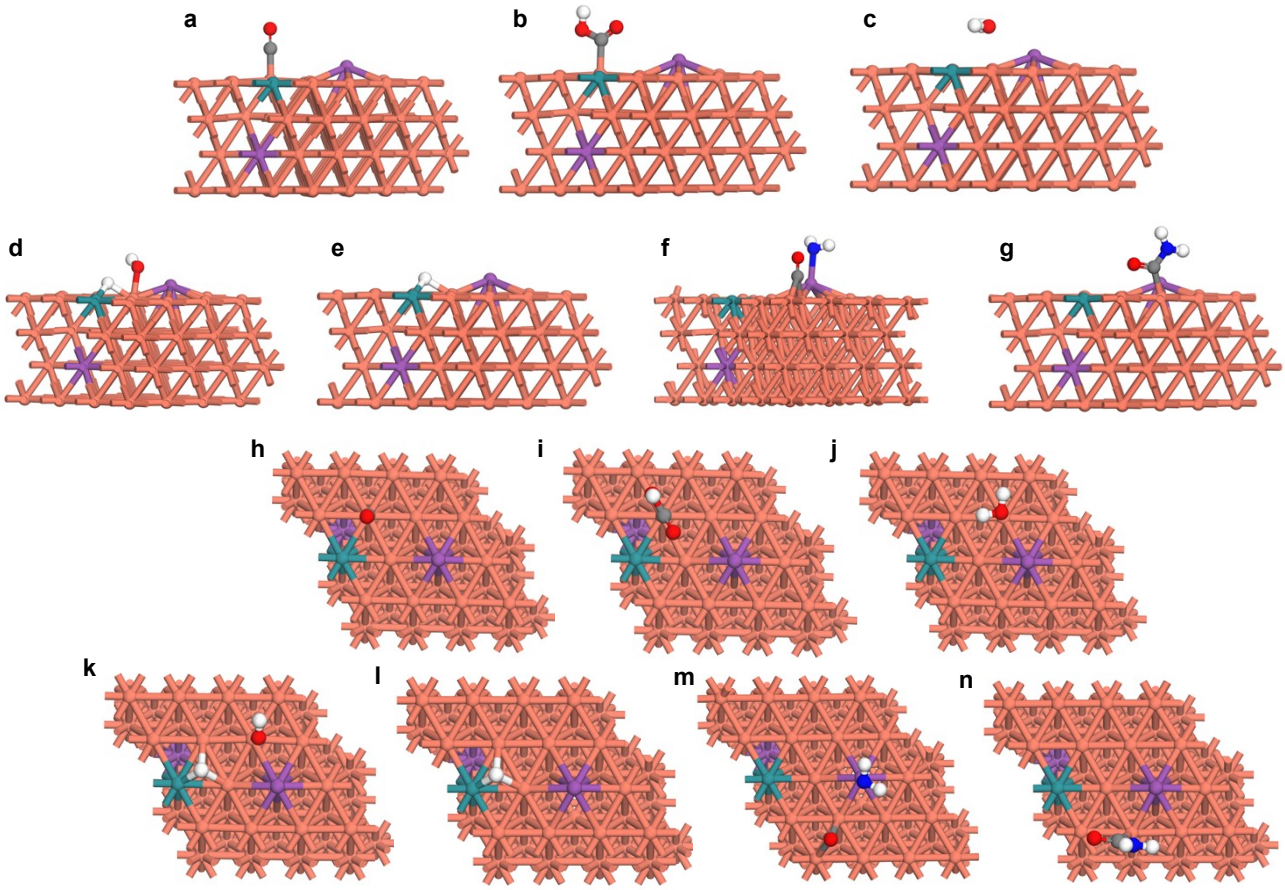

Figure S31. Ru-Cu_9Bi/CNT (111) adsorption of (a, h) *CO, (b, i) *COOH, (c, j) *H_2O, (d, k) *H+*OH, (e, l) *H, (f, m) *CO+*NH_2 and (g, n) *$CONH_2$. Side view (top) and top view (bottom).

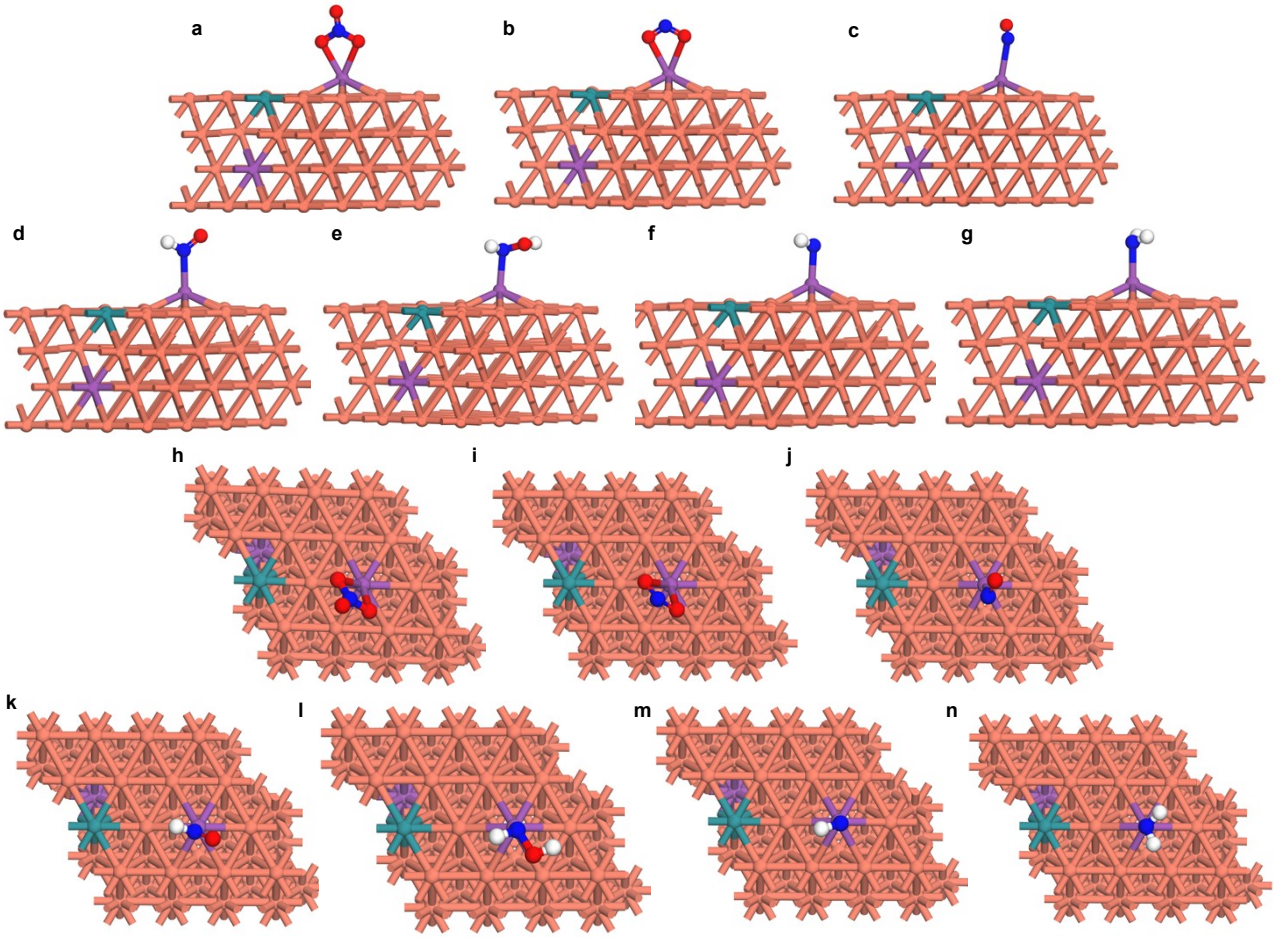

Figure S32. Ru-Cu_9Bi/CNT (111) adsorption of (a, h) *NO_3, (b, i) *NO_2, (c, j) *NO, (d, k) *NHO, (e, l) *NHOH, (f, m) *NH and (g, n) *NH_2. Side view (top) and top view (bottom).

Table S1. Mass ratios of Ru-Cu_xBi_y/CNT with different doping quality characterized by ICP-AES.

	Ru (atom%)	**Cu (atom%)**	**Bi (atom%)**
Ru-Cu_9Bi/CNT	3	87	10
Ru-Cu_7Bi/CNT	4	84	12
Ru-Cu_8Bi/CNT	3	86	11
Ru-$Cu_{10}Bi$/CNT	3	88	9
Ru-Cu_{10}/CNT	5	95	/
Ru-Bi_{10}/CNT	3	/	97

Cu_9Bi/CNT	/	89	11

Table S2. Comparison of the electrocatalytic urea production activity of Ru-Cu_9Bi/CNT with previously reported urea electrosynthesis catalysts in CO_2-saturated $KHCO_3$ + KNO_3

Catalyst	NO_3^- concentration	FE (%)	Yield	Reference
Ru-Cu_9Bi/CNT	**0.01 M**	**65.7**	**40.8 mmol h^{-1} g^{-1}**	**This work**
Ru-Cu_9Bi/CNT	**0.1 M**	**74.8**	**48.8 mmol h^{-1} g^{-1}**	**This work**
Ru-Cu_9Bi/CNT	**1 M**	**75.6**	**61.6 mmol h^{-1} g^{-1}**	**This work**
$In(OH)_3$-S	0.1 M	53.4	8.89 mmol h^{-1} g^{-1}	**Nat. Sustain.**, 2021 (4), 868-876
Vo-InOOH	0.1 M	51.0	9.87 mmol h^{-1} g^{-1}	**ACS Nano**, 2022 (16), 8213-8222
F-CNT-300	0.1 M	18.0	6.36 mmol h^{-1} g^{-1}	**Appl. Catal. B Environ.**, 2022 (316), 121618
Vo-CeO_2-750	0.05 M	/	15.73 mmol h^{-1} g^{-1}	**J. Am. Chem. Soc.**, 2022 (144), 11530-11535
Cu electrodes	0.1 M	3.0	/	**Appl. Catal. B Environ.**, 2022 (316), 121512
Cu-GS-800	0.1 M	28.0	30.0 mmol h^{-1} g^{-1}	**Adv. Energy Mater.**, 2022 (12), 2201500
Graphene-In_2O_3	0.1 M	10.5	5.96 mmol h^{-1} g^{-1}	**Chin. Chem. Lett.**, 2024 (35), 108540
Fe(a)@C-Fe_3O_4/CNTs	0.1 M	16.5	22.35 mmol h^{-1} g^{-1}	**Angew. Chem. Int. Ed.**, 2023 (62), e202210958
PdCu/CBC	0.05 M	69.1	12.73 mmol h^{-1} g^{-1}	**EES Catal.**, 2023 (1), 45-53
Fe-Ni-DASC	0.05 M	17.8	20.2 mmol h^{-1} g^{-1}	**Nat. Commun.**, 2022 (13), 5337
$CuWO_4$	0.1 M	70.9	1.6 mmol h^{-1} g^{-1}	**Nat. Commun.**, 2023 (14), 4491
Cu_1-CeO_2	0.05 M	/	52.84 mmol h^{-1} g^{-1}	**Adv. Mater.**, 2023 (35), 2300020
Vo-S-IO-6	0.1 M	60.6	15.17 mmol h^{-1} g^{-1}	**Appl. Catal. B Environ.**, 2023 (338), 122962
$CoRuN_6$	0.1 M	25.3	8.98 mmol h^{-1} g^{-1}	**Appl. Catal. B Environ.**, 2023 (336), 122917
Pd_4Cu_1-$FeNi(OH)_2$	0.1 M	66.4	436.9 mmol h^{-1} g^{-1}	**Nat. Commun.**, 2023 (14),

				6994
Fe^{II}-$Fe^{III}OOH$@$BiVO_4$	0.1 M	11.5	13.8 mmol h^{-1} g^{-1}	**Appl. Catal. B Environ.**, 2024 (340), 123189
NC	0.1 M	62.0	9.9 mmol h^{-1} g^{-1}	**Nat. Commun.**, 2024 (15), 176
GB-rich Bi	0.1 M	32.0	4.6 mmol h^{-1} g^{-1}	**Angew. Chem. Int. Ed.,** DOI:10.1002/anie.202318589
Co-O-C	0.05 M	31.4	45.07 mmol h^{-1} g^{-1}	***Energy Environ. Sci.***, 2024 (17), 1950-1960

Table S3. The ICP data (mg L^{-1}) of the electrolyte after electro-catalysis test.

Elements	Ru	Cu	Bi
Before reaction	0.0000	0.0000	0.0000
After reaction	0.0004	0.0022	0.0013